Size effects in ferroelectric thin films: 180° domains and polarization relaxation

Rajeev Ahluwalia[1] and David J. Srolovitz[2]
[1]*Institute of Materials Research and Engineering, Singapore 117602, Singapore*
[2]*Department of Physics, Yeshiva University, New York, New York 10033, USA*
(Received 26 September 2007; published 30 November 2007)

The role of 180° domain kinetics on size effects in ferroelectric thin films is studied within a time-dependent Ginzburg-Landau framework. The model incorporates the effect of the depolarization field by considering nonferroelectric-passive layers at the top and bottom surfaces. A critical length scale is predicted below which a depolarization field-induced spontaneous transition from a single domain to a 180° domain pattern causes a time-dependent relaxation of the remnant polarization. This is consistent with the experiments by Kim *et al.* [Phys. Rev. Lett. **95**, 237602 (2005)], where a frequency dependence of the remnant polarization has indeed been observed.

DOI: 10.1103/PhysRevB.76.174121 PACS number(s): 77.80.Dj

I. INTRODUCTION

The properties of nanoscale ferroelectric thin films substantially differ from those in bulk systems.[1] As film thicknesses become progressively smaller, it becomes important to understand the effect of decreasing film thickness on ferroelectric properties. Specifically, is ferroelectricity still retained when the film thickness is as thin as a few unit cells? The bound charges at the electrode-ferroelectric interfaces set up a depolarization field that tends to oppose the polarization. If the bound charges are not compensated, this depolarization field can suppress ferroelectricity below a critical size.[2] The contribution of the electrostatic energy in thin films associated with depolarization fields can be reduced by forming equilibrium 180° domains, leading to the retention of ferroelectricity in films as small as three unit cells.[3] Recent experiments on the switching kinetics of $BaTiO_3$ films have shown that internal depolarization fields can cause relaxation of the remnant polarization P_r during switching.[4] It was suggested that the critical size for ferroelectricity will be influenced by this time-dependent behavior. Thus, kinetics is key to understanding size effects in thin films (incorporating depolarization fields, switching, and 180° domains).

Recently, Dawber *et al.*[5] employed scaling analysis to study the effect of depolarization fields on the size dependence of the coercive field in thin films. This analysis, however, did not account for 180° domains. Bratkovsky and Levanyuk[6] investigated 180° domains by considering a passive (nonferroelectric) layer at the ferroelectric-electrode interface. (Nonferroelectric layers provide incomplete charge compensation at the interface.) They showed that the passive layer stabilizes a 180° domain pattern instead of a single domain state. Although this calculation showed that the 180° domain patterns could strongly modify the physics in thin film ferroelectrics, their influence on size effects and switching kinetics remains unexplored. Tagantsev *et al.* studied the effects of passive layers on the switching loops, but here too kinetic and domain wall motion effects were not incorporated.[7]

Motivated by the experiments in Ref. 4, our aim in this paper is to understand the role played by the kinetics of 180° domains on size effects in ferroelectric thin films. We show how domain wall motion increasingly influences the polarization-electric field (P-E) curves as the film thickness is reduced to a few nanometers. We address these issues by combining the passive layer model and a time-dependent Ginzburg-Landau (TDGL) approach that describes kinetic effects. The TDGL equations have been widely used to study domain evolution and switching in ferroelectrics,[8–10] but the effect of 180° domains on size effects has not been investigated.

In this paper, we focus on the basic physics of depolarization fields and 180° domains in very thin films. This necessarily implies that several simplifying assumptions were made. For example, we ignore disorder associated with static defects in the material.[11,12] Similarly, the effects of thermal fluctuations have also been neglected. At small thicknesses, the physics is dominated by strong depolarization fields, such that thermal fluctuations and static defects should play a relatively small role. These simplifications also allow us to study effects that are purely due to depolarization fields. For computational simplicity, we also restrict to a two-dimensional (2D) system. While this approximation may quantitatively influence the kinetics and the critical thicknesses, the qualitative physics is expected to be independent of the dimensionality.

The organization of this paper is as follows. In Sec. II, we give the details of the passive layer model. Section III presents the detailed results of the simulations, including domain patterns and polarization switching as a function of film thickness and switching frequency. Finally, in Sec. IV, we summarize the main results of the paper and discuss their implications.

II. MODEL

We consider a ferroelectric film of thickness h ($|z| \leqslant h/2$) with passive (i.e., dielectric) layers of thickness d at the top and bottom surfaces. We assume that the film is c axis oriented and, hence, the polarization normal to the film surface P_z is the appropriate order parameter. This means that 90° domains cannot form in the present model. The total free energy is given as $F_T = F + F_{dep}$, where

$$F = \begin{cases} \int d\vec{r}\left[\alpha_0(T-T_0)P_z^2 - \beta P_z^4 + \gamma P_z^6 + \frac{K}{2}(\nabla P_z)^2 + \frac{1}{2\chi_{xx}}P_x^2\right], & |z| \leq \frac{h}{2} \\ \int d\vec{r}\left[\frac{1}{2\chi_p}(P_x^2 + P_z^2)\right], & \frac{h}{2} < |z| \leq \frac{h}{2} + d. \end{cases} \quad (1)$$

For $|z| \leq h/2$, the above equation represents a ferroelectric in which P_z, the polarization normal to the film surface, is the order parameter. A harmonic term in P_x, the polarization in the lateral direction, is also included to allow for the rotation of the polarization vector in the x-z plane. The quantities α_0, T_0, β, γ, and K are material specific parameters that describe the ferroelectric transition. χ_{xx} is the susceptibility in the direction parallel to the film surface, x. For $h/2 < |z| \leq (h/2 + d)$ (inside the passive layers), the free energy is that of an isotropic linear dielectric with susceptibility χ_p. The depolarization energy associated with the film is given by

$$F_{dep} = -\int d\vec{r}\left[\frac{\varepsilon_0}{2}(\vec{E}_{dep}\cdot\vec{E}_{dep}) + \vec{E}_{dep}\cdot\vec{P}\right], \quad (2)$$

where the depolarization field is related to the potential ϕ by $E_{dep} = -\vec{\nabla}\phi$. The boundary conditions for the film are $\partial P_z/\partial z = 0$ at $|z| = h/2 + d$. The potential is specified at the surfaces as $\phi = -V/2$ at $z = h/2 + d$ and $\phi = V/2$ at $z = -(h/2 + d)$, where V is the applied voltage across the film. Further, the Maxwell equation $\vec{\nabla}\cdot\vec{D} = 0$ ($\vec{D} = \varepsilon_0\vec{E} + \vec{P}$) gives rise to the constraint

$$-\varepsilon_0\nabla^2\phi + \vec{\nabla}\cdot\vec{P} = 0. \quad (3)$$

It is clear from Eq. (3) that a nonzero value of $\vec{\nabla}\cdot\vec{P}$ at the ferroelectric-passive layer interface can result in the creation of a depolarization field inside the film.

The TDGL equations for the evolution of the polarization are

$$\frac{\partial P_i}{\partial t} = -\Gamma\frac{\delta F_T}{\delta P_i}, \quad i = x,z, \quad (4)$$

where Γ is related to the domain wall mobility and sets the simulation time scale.

III. SIMULATIONS OF DOMAIN PATTERNS AND POLARIZATION SWITCHING

The TDGL equations in Eq. (4) are solved using finite differences such that the constraint in Eq. (3) is satisfied at all times and at all points in space. The parameters were chosen to be appropriate for a $BaTiO_3$ single crystal,[13] $\alpha_0 = 3.34 \times 10^5$ V m/C, $T_0 = 381$ K, $\beta = 6.381 \times 10^8$ V m^5 C^{-3}, $\gamma = 7.89 \times 10^9$ V m^9 C^{-5}, and $K = 1.38 \times 10^{-11}$ V m^3 C^{-1}, and the temperature was set to $T = 300$ K. The susceptibilities are chosen as $\chi_{xx} = 417\varepsilon_0$ and $\chi_p = 208\varepsilon_0$ for illustrative purposes. The simulations are performed in 2D using finite difference methods with a simulation cell that is periodic along the x direction and the condition $\partial P_z/\partial z = 0$ at $z = \pm(h/2 + d)$. The smallest length scale in the simulations is $\delta = 0.71$ nm and the lateral width is $L = 177.5$ nm. The thickness of the passive layer is fixed at $d = 7.1$ nm, while the film thickness is varied in the range 7.1 nm $\leq h \leq$ 145.55 nm.

We first study the formation of domain structures following a quench from the paraelectric phase, as a function of the film thickness h. Time is measured in the rescaled units, $t^* = (81\alpha_0\Gamma)t$. The paraelectric state is simulated by initializing $P_x(\vec{r}, t=0)$, $P_y(\vec{r}, t=0)$, and $\phi(r, t=0)$ with small amplitude random fluctuations around zero. We use short circuit boundary conditions, i.e., $\phi(x, z = h/2 + d) = \phi[x, z = -(h/2 + d)] = 0$. Equations (3) and (4) are used together with these boundary conditions to simulate the formation and the evolution of the domain structures. Figure 1 shows the simulated domain patterns in films of thicknesses $h = 60.35$ nm, $h = 24.85$ nm, and $h = 7.1$ nm. The corresponding depolarization field $E_z = -(\partial\phi/\partial z)$ is shown in Fig. 2. It is clear that domain formation shields the bulk of the film from the depolarization field, which is localized at the ferroelectric-passive layer interface. However, as the thickness is reduced, the surface fields from the top and bottom nearly overlap, thereby raising the electrostatic energy. This high electrostatic energy completely suppresses the ferroelectric phase below $h = 7.1$ nm. Thus, Figs. 1(c) and 2(c) correspond to critical size ($h = 7.1$ nm) below which the film becomes paraelectric.

Next, we study the effect of changing the film thickness on the polarization switching process. At first, the method

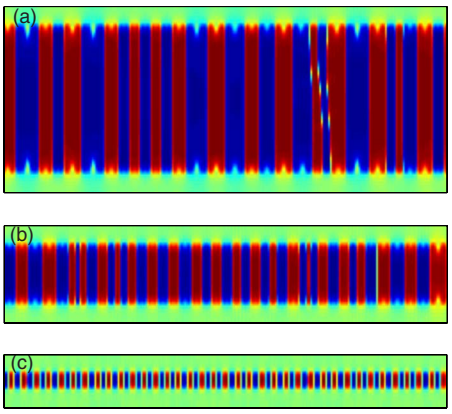

FIG. 1. (Color online) Domain patterns for films with thicknesses (a) $h = 60.35$ nm, (b) $h = 24.85$ nm, and (c) $h = 7.1$ nm. The passive layer width $d = 7.1$ nm and the lateral size of the simulation cell $L = 177.85$ nm are kept fixed. The polarization in the domains varies between $P_z = 0.26$ C m^{-2} (red) and $P_z = -0.26$ C m^{-2} (blue), while $P_z \cong 0$ inside the passive layer (green).

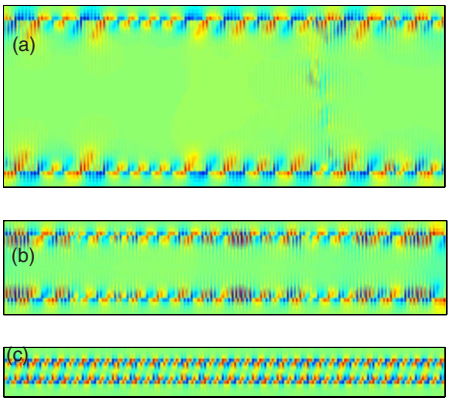

FIG. 2. (Color online) The distribution of the depolarization field E_z corresponding to Fig. 1. E_z varies between (a) ±1200 kV/cm, (b) ±1100 kV/cm, and (c) ±590 kV/cm, where ± limits are shown in red (blue) (green corresponds to $E_z=0$).

used to obtain the domain structures of Fig. 1 is repeated but this time with an applied voltage $\phi[x,z=\pm(h/2+d)] = \mp V_m/2$. We refer to this process as field cooling. The configuration formed after this process is then subjected to a time-dependent potential $\phi[x,z=\pm(h/2+d)] = \mp(V_m/2)\cos(\omega^* t^*)$ to simulate the switching process, where ω^* is the switching frequency. The *P-E* loops are determined by plotting the instantaneous average electric field $\langle E_z\rangle$ inside the entire composite system versus the instantaneous average polarization $\langle P_z\rangle$ calculated inside the ferroelectric.

Figure 3 shows the calculated *P-E* curves for films with thicknesses $h=145.55$ nm, $h=60.35$ nm, and $h=7.1$ nm at a switching frequency of $\omega^*=3.14\times10^{-6}$ and potential V_m

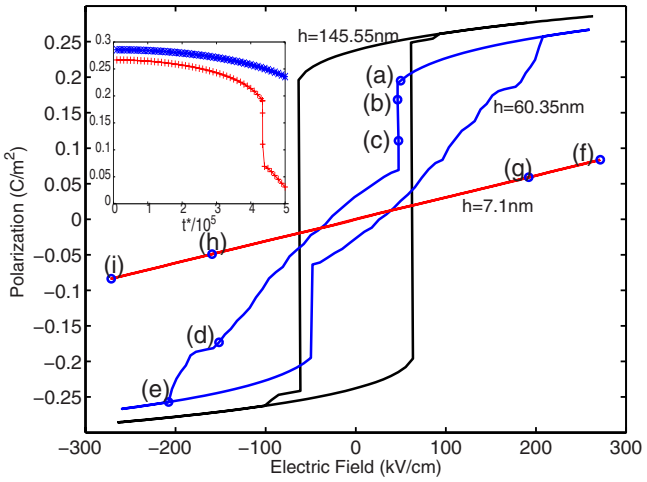

FIG. 3. (Color online) Simulated *P-E* curves at $\omega^*=3.14\times10^{-6}$ for three different film thicknesses. The domain patterns corresponding to points (b)–(d) are shown in Fig. 4 and for (f)–(i) in Fig. 5. Point (a) for $h=60.35$ nm corresponds to the unswitched single domain state with $P_z>0$ and (e) to a fully switched single domain with $P_z<0$. The inset shows the corresponding P_z vs t^* plot for $h=145.55$ nm (blue) and $h=60.35$ nm (red) as the applied potential is reduced to zero.

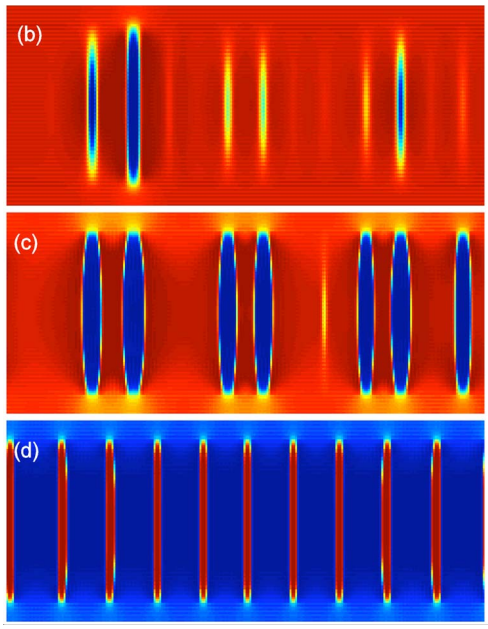

FIG. 4. (Color online) Domain patterns for $h=60.35$ nm, corresponding to points (b)–(d) in Fig. 3. The color scheme is as in Fig. 1.

chosen such that $\langle E_z^{\max}\rangle\sim260$ kV/cm for all thicknesses. Note the large *P-E* loop shape change that occurs with changes in the ferroelectric film thickness. For $h=145.55$ nm, the usual square loop with a stable single domain remnant state is obtained. However, the switching process is not entirely homogeneous and 180° domains do appear in the coercive region of the *P-E* loop. The drastic *P-E* loop shape change for smaller thicknesses can be understood by examining the domain evolution in Figs. 4 and 5. The domain patterns corresponding to points (b)–(d) in Fig. 3 are shown in Fig. 4 for $h=60.35$ nm [(a) and (e) correspond to single domain states]. For this case, the field cooling at $\langle E_z^{\max}\rangle=260$ kV/cm results in a single domain state with $P_z>0$. As the electric field is reversed, there is a depolarization-induced single domain to multidomain transition at a critical field which leads to a jump in the *P-E* curve. The transition occurs by the formation of the reversed polarization domains in the middle of the film. Thereafter, as the

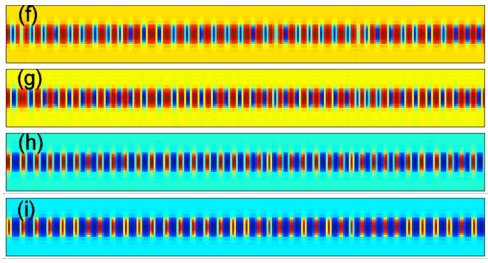

FIG. 5. (Color online) P_z domain patterns for $h=7.1$ nm, corresponding to points (f)–(i) in Fig. 3. The motion of domain walls can be inferred by the fact that the red domains are thicker in (f), whereas the blue domains are thicker in (i). The colors in the passive layers correspond to $P_z=0.0832$, 0.0585, −0.052, and −0.0832 C m^{-2} for (f)–(i).

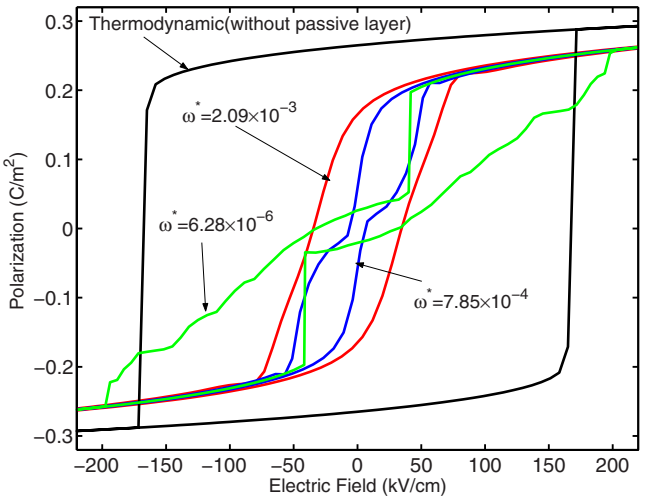

FIG. 6. (Color online) Simulated *P-E* loops for the $h=63.9$ nm film at three different switching frequencies. The appropriate thermodynamic switching loop for a system without passive layers is also shown for comparison.

field is further decreased, the reversed domains grow by sideway motion and eventually a single domain of the reversed polarization is obtained. This depolarization-induced domain formation and the domain wall motion are responsible for the unusual shape of the *P-E* curve.

At small thicknesses ($h<24.85$ nm), the depolarization effect is so strong that for the same applied external field $\langle E_z^{\max}\rangle=260$ kV/cm, 180° domains are observed instead of a single domain after field cooling. In these cases, the switching process may be described as the back and forth sideway motion of the domain walls, as seen in Fig. 5 for the $h=7.1$ nm thick film.

The shape change of the *P-E* loops from "squarish" at larger thicknesses to "tilted" at lower thicknesses is qualitatively consistent with recent experiments on $BaTiO_3$ films.[14] However, in Ref. 14, the abrupt jumps in the loops have not been observed. Figure 6 shows that for higher switching frequencies, we obtain the usual continuous loops; in these cases, there is insufficient time for the domain pattern to develop completely. This suggests that the unusual loops observed here may be experimentally observed for very slow switching and small film thicknesses.

Figure 6 shows the simulated hysteresis loops for $h=63.9$ nm for three different frequencies. The thermodynamic switching loop for a system with no passive layer is also plotted. The "coercive field paradox" states that the experimental coercive fields are much lower than the thermodynamic coercive fields and this reduction cannot be explained on the basis of thermal nucleation of domains.[15] It is clear from Figs. 3 and 6 that a significant reduction in the coercive field compared to the thermodynamic coercive field is observed. Since no thermal fluctuations and defects have been included in the model, this reduction is purely due to the depolarization fields and the associated 180° domain formation. This suggests that depolarization-induced domain formation in thin films may play an important role in making experimentally observed coercive fields much lower than the corresponding thermodynamic coercive fields. Figure 6 also suggests that the remnant polarization P_r depends on the switching frequency. The frequency dependence of P_r is due to the fact that in the absence of an external field, a single domain state becomes unstable below a critical thickness of $h=86.62$ nm. The existence of this critical thickness can also be seen in Fig. 3 where a stable single domain remnant state is observed for the $h=145.55$ nm film, whereas the remnant polarization for the $h=60.35$ nm film is significantly reduced due to domain formation depicted in Fig. 4. For $h<86.62$ nm, a single domain state will evolve in time to form a multidomain state resulting in a dynamic relaxation of the remnant polarization. Thus, we find a critical thickness below which the remnant polarization becomes frequency dependent (note that this critical thickness is higher than the critical thickness of $h=7.1$ nm below which the film becomes paraelectric). In fact, frequency dependence of P_r has indeed been observed for very thin $BaTiO_3$ films by Kim *et al.*[4]

IV. DISCUSSION AND SUMMARY

We have examined ferroelectric film thickness effects within the framework of a TDGL model, incorporating both the effects of depolarization fields and 180° domains. We demonstrated that depolarization-induced 180° domain formation strongly modifies the ferroelectric behavior of nanoscale films. It is shown that this domain formation leads to a significant reduction of the coercive field compared to the thermodynamic coercive field. A new length scale is found below which a single domain remnant state becomes unstable and splits into 180° domains. Below this critical thickness, there is a spontaneous transition from a single domain to multidomain state as the electric field is reversed. This transition is responsible for the relaxation and frequency dependence of the remnant polarization. An important conclusion is that the critical size for ferroelectricity in thin films is not a purely thermodynamic quantity but is also influenced by the kinetics and switching frequency. We note that the previous analytical approaches[6,7] are not capable of capturing such important kinetic effects. The present calculation underscores the importance of using a kinetic approach to understand the physics of ferroelectric thin films, particularly in light of recent experiments[4] that show that time-dependent effects become very important on the nanoscale.

ACKNOWLEDGMENTS

We gratefully acknowledge useful discussions with Nikolai Yakovlev and the A-Star VIP programme for financial support.

[1] M. Dawber, K. M. Rabe, and J. F. Scott, Rev. Mod. Phys. **77**, 1083 (2005).
[2] J. Junquera and P. Ghosez, Nature (London) **422**, 506 (2003).
[3] S. K. Streiffer, J. A. Eastman, D. D. Fong, C. Thompson, A. Munkholm, M. V. Ramana Murty, O. Auciello, G. R. Bai, and G. B. Stephenson, Phys. Rev. Lett. **89**, 067601 (2002).
[4] D. J. Kim, J. Y. Jo, Y. S. Kim, Y. J. Chang, J. S. Lee, Jong-Gul Yoon, T. K. Song, and T. W. Noh, Phys. Rev. Lett. **95**, 237602 (2005).
[5] M. Dawber, P. Chandra, P. B. Littlewood, and J. F. Scott, J. Phys.: Condens. Matter **15**, L393 (2003).
[6] A. M. Bratkovsky and A. P. Levanyuk, Phys. Rev. Lett. **84**, 3177 (2000).
[7] A. K. Tagantsev, M. Landivar, E. Colla, and N. Setter, J. Appl. Phys. **78**, 2623 (1995).
[8] W. Zhang and K. Bhattacharya, Acta Mater. **53**, 185 (2005).
[9] J. Wang and T. Y. Zhang, Phys. Rev. B **73**, 144107 (2006).
[10] S. Choudhury, Y. L. Li, C. E. Krill III, and L. Q. Chen, Acta Mater. **53**, 5313 (2005).
[11] A. Gruverman, B. J. Rodriguez, C. Dehoff, J. D. Waldrep, A. I. Kingon, R. J. Nemanich, and J. S. Cross, Appl. Phys. Lett. **87**, 082902 (2005).
[12] A. Grigoriev, D. Y. Do, D. M. Kim, C. B. Eom, B. Adams, E. M. Dufresne, and P. G. Evans, Phys. Rev. Lett. **96**, 187601 (2006).
[13] R. Ahluwalia, T. Lookman, A. Saxena, and W. Cao, Phys. Rev. B **72**, 014112 (2005).
[14] Y. S. Kim, D. H. Kim, J. D. Kim, Y. J. Chang, T. W. Noh, J. H. Kong, K. Char, Y. D. Park, S. D. Bu, J. G. Yoon, and J. S. Chung, Appl. Phys. Lett. **86**, 102907 (2005).
[15] G. Gerra, A. K. Tagantsev, and N. Setter, Phys. Rev. Lett. **94**, 107602 (2005).